SPHERICAL EXOSKELETON FOR THE MEASUREMENT OF SHOULDER MOVEMENT

Jiaji Li[1], John Golden[1], Bailey E. Johnson[2], Edward Quilligan[2],
Vance O. Gardner[2], Carlos A. Prietto[2], J. Michael McCarthy[1]
[1]*Robotics and Automation Laboratory, University of California, Irvine, Irvine, CA, USA 92697*
Email: jiajil5@uci.edu; jtgolden@uci.edu; jmmccart@uci.edu
[2]*Hoag Orthopedics, Irvine, Irvine CA, USA*
Email: Bailey.Johnson@hoag.org; edward.quilligan@hoagorthopedics.org; vogardner@gmail.com; cprietto2@gmail.com

ABSTRACT

This paper presents the design, construction and testing of a spherical shoulder exoskeleton that measures shoulder movement for use before and after shoulder replacement surgery, known as total shoulder arthroplasty. The device is designed for in-home use to facilitate remote physiotherapy. Embedded sensor data is converted to a robotic shoulder model to illustrate the measured movement and which is validated through ImageJ measurements. Unlike current motion capture and image processing measurement techniques, this device measures the movement of the upper arm relative to the scapula, excluding scapula movement, thereby focusing on movement provided by the shoulder prosthesis.

Keywords: spherical exoskeleton; shoulder range of motion; ImageJ; goniometer.

EXOSQUELETTE SPHÉRIQUE POUR LA MESURE DU MOUVEMENT DE L'ÉPAULE

RÉSUMÉ

Cet article présente la conception, la construction et les essais d'un exosquelette sphérique qui mesure les mouvements de l'épaule avant et après l'arthroplastie totale de l'épaule. L'appareil est conçu pour être utilisé à domicile afin de faciliter la physiothérapie à distance. Les données des capteurs intégrés sont converties en un modèle d'épaule robotisée pour illustrer le mouvement mesuré, et comparées aux mesures d'ImageJ. Contrairement aux techniques actuelles de capture de mouvement et de traitement d'images, ce dispositif mesure le mouvement du bras par rapport à l'omoplate, à l'exclusion du mouvement de l'omoplate, se concentrant ainsi sur le mouvement fourni par la prothèse de l'épaule.

Mots-clés : exosquelette sphérique ; amplitude de mouvement des épaules ; ImageJ ; goniomètre.

1. INTRODUCTION

In this paper, we introduce an instrumented exoskeleton designed to measure shoulder range of movement in order to assess performance after surgical replacement of a shoulder joint (total shoulder arthroplasty). See Fig. 1. The structure used for our device was inspired by the movable shoulder brace described by Castro et al. [1, 2]. It is a spherical scissor mechanism consisting of six bars configured to form two spherical rhombus diamonds, with the central bars crossed to form scissors. See Fig. 2. The axes of the seven joints intersect at the center of the shoulder so that the links move on spheres around the shoulder.

The shoulder joint is formed by connections between the upper arm bone (humerus) to both the shoulder blade (scapula) and the collar bone (clavicle) and involves a number of structures and muscles that support the shoulder and allow a large range of movement. The measurement of the angular movement of the shoulder is performed by a therapist using a specialized protractor known as a goniometer; other methods for joint measurement are described in the literature review.

The goal of this paper is to present the analysis that transforms the angular measurements of our exoskeleton into angular values for a shoulder joint simulation in order to compare with those obtained from ImageJ. A prototype device was used to measure shoulder joint range of movement of the authors as a preliminary assessment of its usefulness.

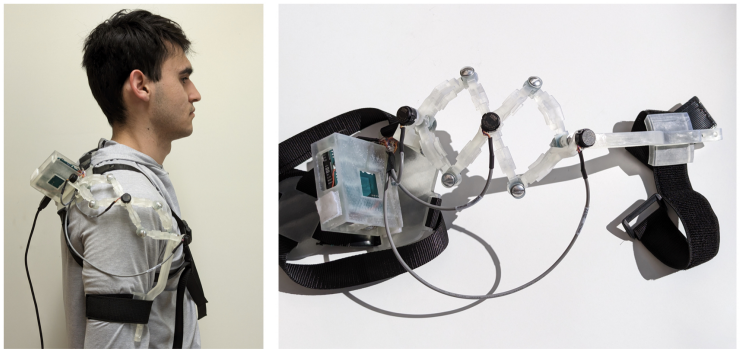

Fig. 1. The spherical exoskeleton system mounted on the shoulder of a patient to measure the movement of the upper arm relative to the scapula.

2. LITERATURE REVIEW

In home measurement of motion of the upper arm that is transmitted to remote physiotherapy services can be used to motivate and monitor a rehabilitation plan in a manner that is more convenient for the patient. In order to track and motivate adherence to the rehabilitation plan, Munoz et al. [3] use a Microsoft Kinect V2 motion capture system connected to a specially designed video game.

A comparison of Kinect-based motion capture to the results of four Optitrack cameras was performed by Bilesan et al. [4], who use a robot as the ground truth for comparison. The use of a simplified mechanical model of the shoulder joint as a ball and socket was shown by Krishnan et al. [5] to extend to over 200 research papers, despite the known translations and rotational asymmetries introduced by the clavicle and scapula as well as shoulder ligaments and girdle. A more detailed model of shoulder movement introduced by Lenarcic et al. [6] defines upper arm movement as the result of a kinematic chain of seven joints connected to the spine.

Another approach to the measurement of shoulder movement uses video image processing. Gauci et al. [7] found that the analysis of video images from an RGB-D camera, which records separate color images as well as the distance to the object, yielded good agreement for shoulder measurement when compared to

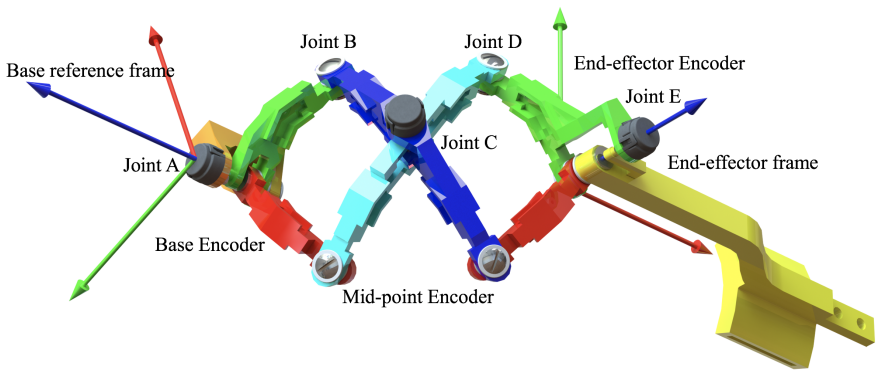

Fig. 2. A solid model of the spherical exoskeleton system that shows the spherical scissor mechanism that wraps around the shoulder of the patient.

goniometry. Tanioka et al. [8] used 2D video images analyzed by ImageJ, an open source image processing software available through the National Institute of Mental Health, in order to evaluate the shoulder range of movement during their patient's upper limb exercises. They found that their video measurements were in good agreement with a goniometer. However, they also noticed that there was significant difference between active and passive range of movement. Apparently, some of their patients had limited active range of movement that was not measured by the goniometer, and they used compensatory movements to expand this range of movement when exercising.

Park et al. [9] uses a two-link robot arm to measure shoulder movement, which shows close similarities with angular measurement obtained from images evaluated using ImageJ. This requires measurement in a clinical setting. In contrast, our spherical exoskeleton can be put into place by the patient in a manner similar to putting on a coat. This device is instrumented so that movement is recorded without image processing.

Because total shoulder arthroplasty, also known as reverse shoulder replacement, attaches a mechanical socket to the upper arm that fits over a ball mounted on the shoulder blade, our spherical exoskeleton is designed to measure the rotational movement of the upper arm relative to the scapula. This directly assesses the range of motion associated with shoulder joint replacement surgery. The system can be used by the patient at home as part of telerehabilitation assessment.

3. FABRICATION OF THE EXOSKELETON

3.1. Additive manufacture

The spherical exoskeleton was modeled in SolidWorks 2022 (Dassault Systémes, Vélizy-Villacoublay, France), Fig. 2. Motion analysis demonstrated the movement of the device in coordination with the arm of a humanoid figure. This provided the initial verification of the design.

The solid model of the prototype consists of 11 parts to be manufactured by 3D printing. The parts were transformed to .stl files by the slicing software Chitubox (Chitubox, Shenzhen, Guangdong, China). The sliced files were transferred and adjusted for the Photon Mono X (Anycubic, Shenzhen, Guangdong, China), an LCD-based SLA that would give ±100 µm x-y resolution, which provided smooth movement of the device. The Anycubic Wash and Cure Plus system was used to finalize the fabrication, Fig. 3.

3.2. Exoskeleton assembly

The movement of the exoskeleton is provided by hinges formed from 3/16 in. diameter aluminum binding posts with three #10 washers between crevices for smoother actuation. Three micro optical encoders (US Digital, Vancouver, WA, USA) are mounted on the center joints of the exoskeleton. The encoder base is

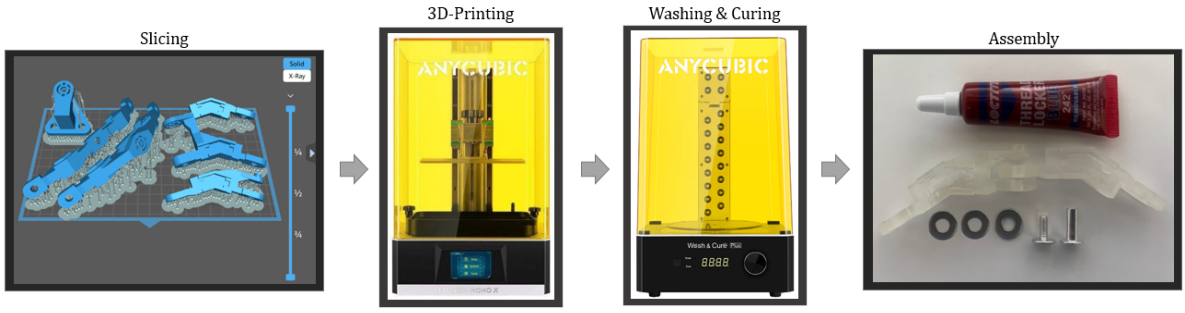

Fig. 3. The fabrication sequence consists of (i) slicing the model, (ii) 3D printing the parts, (iii) washing and curing the parts, and (iv) assembly of the parts. (Image of Photon Mono X and Cure and Wash Station)

attached to one link while the drive shaft is inserted and glued to a fitted hole in the moving link. The base of the system holds the Arduino Uno (Arduino, Turin, Piedmont, Italy), which processes the encoder signals. The entire device is supported by a wearable rigging made of nylon straps and plastic clips, Fig. 1.

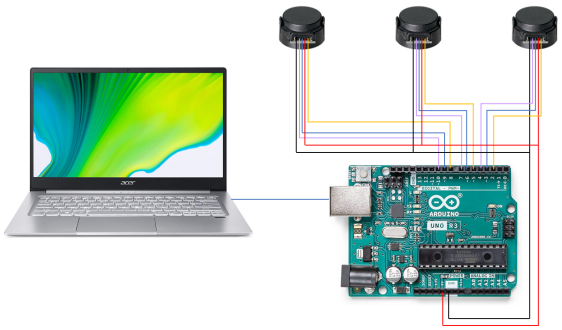

Fig. 4. An Arduino Uno collects the optical sensor data and transfers it to MATLAB on a computer to calculate arm movement.

The layout for the electronics of this system is shown in Fig. 4. The optical encoders return 1024 pulses for 360 degrees of rotation. The code reads both the pulse and spacing between pulses, thus giving 2048 counts per 360 rotation. These encoders are designated as A for the measurement of the rotation relative to the base joint, C for measurement of the relative rotation of the two center links, and E for measurement of the movement of the end link. See Fig. 5.

Encoder Angle	Pulse Variation	Measured Angle
A.1	±3	74.11°
A.2	±2	167.33°
C.1	±9	32.98°
C.2	±8	130.15°
E.1	±0	53.78°
E.2	±3	236.37°

Table 1. Arduino pulse range and extracted ImageJ angles.

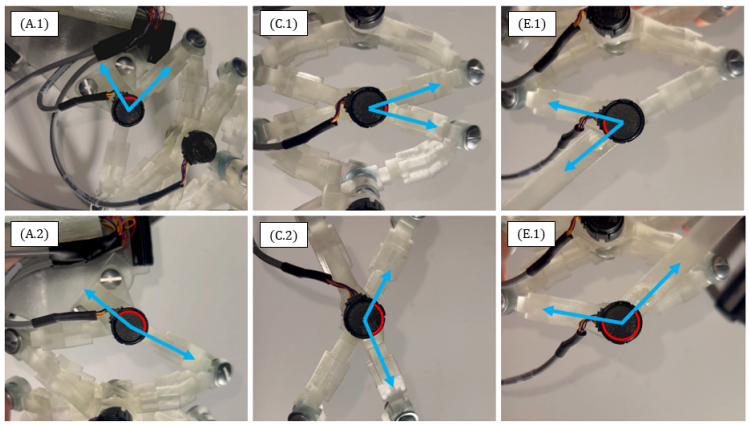

Fig. 5. The minimum and maximum values for each of the optical encoders at joints **A**, **C** and **E** were measured before mounting the exoskeleton on a patient.

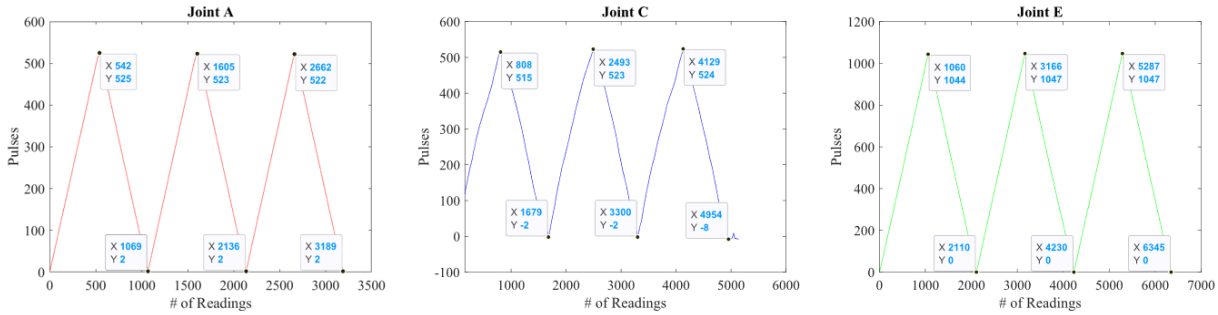

Fig. 6. Measurements of maximum and minimum pulse values obtained for each of the optical encoders.

3.3. Calibration

The exoskeleton has hard stops at minimum and maximum range of extension. The measurement of the optical encoders at these points are shown in Fig. 5 and listed in Table 1. An example measurement is shown in Fig. 6, which shows the device contracted to its minimum dimension and expanded to its maximum dimension three times. Pulse counts were measured and matched to external angular measurements.

The values of the minimum and maximum pulses at each optical encoder provide the mean and variation of the sensor output. A video camera was mounted to record the movement of the exoskeleton from minimum to maximum extension. Screenshots taken by Bandicam (Bandicam Company, Irvine, CA, USA) were transferred to GIMP image processing (Open Source) and used to find the center-most pixel between the linkages and the encoder. ImageJ (National Institute of Health, Bethesda, MD, USA) was used to evaluate the angular position associated with the minimum and maximum joint angles.

In order to eliminate the count variation associated with the microprocessor due to the large input of sensor data or vibration of the shaft in the encoder. The resulting calibration for each of the optical encoders is shown in Table 2, which shows that there are approximately five pulses per degree of rotation for each of the sensors. The variation of these calibrated values shows that our microprocessor has dropped counts, despite this the calibration yielded reliable results at low angular velocities.

Encoder	Mean Pulse Count	Measured Angle $\Delta\theta$	Calibrated $\frac{pulse}{degree}$
A	522	93°	5.613
C	518	97°	5.340
E	1046	183°	5.716

Table 2. The calibration of pulse count to ImageJ angle measurements.

4. KINEMATICS ANALYSIS

4.1. Overview

In order to obtain the angles of the upper arm movement of a patient relative to the torso from data measured by the exoskeleton, we use a robotic shoulder model, known as an RR serial chain. The position of the patient's arm measured by the exoskeleton yields a coordinate transformation matrix $[\mathbf{T}]$. The kinematic model of the RR shoulder, $[\mathbf{B}(\phi_1, \phi_2)]$, must equal this transformation, and therefore provide formulas to determine the angles that define the position of the arm. See Fig. 7.

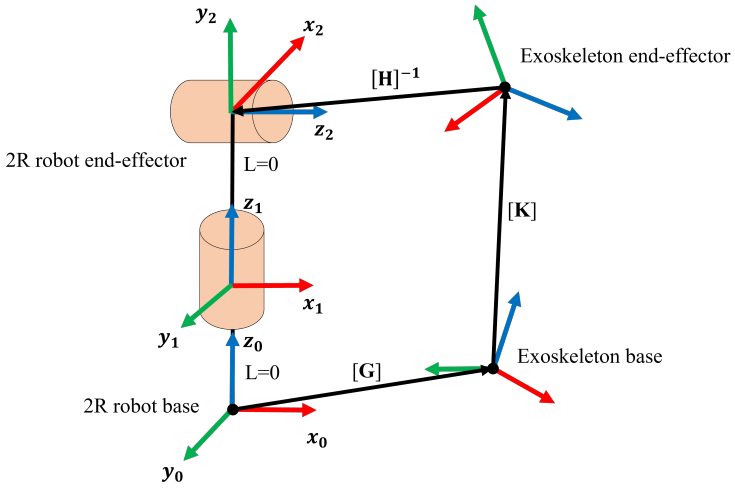

Fig. 7. The coordinate transformations that relate the position of the robot model of the shoulder to the kinematic model of the exoskeleton.

To achieve this objective, the base frame of the exoskeleton is transformed to the base frame of the RR robot, while the end-effector frame of the exoskeleton is transformed to the end-effector frame of the RR robot. These two transformations are constant as long as the exoskeleton remains fixed on the tester's shoulder. Therefore, the kinematic equation from the RR robot's base frame to its end-effector can be expressed as

$$[\mathbf{T}] = [\mathbf{G}][\mathbf{K}][\mathbf{H}]^{-1}, \tag{1}$$

where $[\mathbf{G}]$ represents the transformation from the exoskeleton's base frame to the RR robot's base frame, $[\mathbf{K}]$ represents the kinematic transformation from the exoskeleton's base frame to its end-effector, and $[\mathbf{H}]$ represents the transformation from the exoskeleton's end-effector frame to the RR robot's end-effector frame.

4.2. Kinematics Equations

The spherical shoulder exoskeleton is a 3-degrees-of-freedom (DOF) manipulator consisting of a ternary base link, two spatial rhombuses, and a binary link. The two rhombuses form a scissor mechanism, where

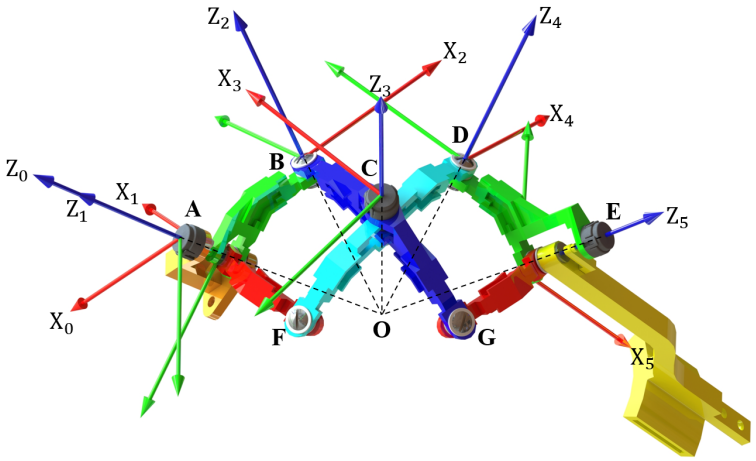

Fig. 8. The joint coordinate frames used to model the kinematics of the spherical shoulder exoskeleton. These frames are located at shoulder center, **O**, but have been positioned at the joints for visualization.

all revolute joints are at the same spherical surface, and all the rotational axes pass through the spherical center **O**. The kinematic analysis is performed by analysing the serial chain formed by joints **A**, **B**, **C**, **D** and **E**, which is constrained by the two rhombus linkage **ABCF** and **CDEG**, Fig. 8. The result is a five-jointed serial chain, Table 3, with joints θ_2 and θ_4 defined by the value of joint θ_3.

The base frame of the device, denoted by $X_0Y_0Z_0$, is located on the surface of the first sensor, while the end-effector frame, denoted by $X_5Y_5Z_5$, is aligned with the binary link on the exoskeleton. The rest of the frames are at the spherical center **O**. The Denavit-Hartenberg (DH) parameters of the exoskeleton, presented in Table 3, are based on the fact that all the rotational axes twist 35° [1].

Axis i	Angle θ_i	Link offset d_i	Twist $\alpha_{i,i+1}$	Link length $r_{i,i+1}$
1	θ_1	−122.98 mm	35°	0
2	θ_2	0	35°	0
3	θ_3	0	35°	0
4	θ_4	0	35°	0
5	θ_5	85.06 mm	0	0

Table 3. The Denavit-Hartenberg (DH) parameters of the exoskeleton.

Let $[\mathbf{A}_i]$ denote the homogeneous transformation matrix for each link of the exoskeleton, which is obtained from DH table, Table 3, given by,

$$[\mathbf{A}_i] = [\mathbf{Z}(\theta_i, d_i)][\mathbf{X}(\alpha_{i,i+1}, r_{i,i+1})], \tag{2}$$

where $[\mathbf{Z}(\theta_i, d_i)]$ is the coordinate screw displacement about the z-axis by the angle θ_i and slide d_i, and $[\mathbf{X}(\alpha_{i,i+1}, r_{i,i+1})]$ is the coordinate screw displacement about the x-axis by the angle $\alpha_{i,i+1}$ and slide $r_{i,i+1}$.

Using this definition of the link transformations $[\mathbf{A}_i]$, the DH table yields the kinematics equation of the exoskeleton as,

$$[\mathbf{K}] = [\mathbf{A}_1(\theta_1)][\mathbf{A}_2(\theta_2)][\mathbf{A}_3(\theta_3)][\mathbf{A}_4(\theta_4)][\mathbf{A}_5(\theta_5)], \tag{3}$$

where θ_i are variable joint angles.

The joint angles θ_1, θ_3 and θ_5 are measured by optical encoders A, C, E, respectively. Joint angles θ_2 and θ_4 can be computed using the geometry of the exoskeleton.

4.3. Exoskeleton Geometry

The spherical shoulder exoskeleton has the geometry of a scissor mechanism wrapped onto the surface of a sphere. This results in spherical quadrilaterals that can be analyzed using the geometry of spherical four-bar linkages presented by Chiang (1992)[10]. The relationship between input and output angles of a spherical four-bar linkage is also presented by Hayes et al. (2023)[11]. Here we compute the input-output equations of the rhombus **CDEG** using the equations in McCarthy and Soh (2010)[12].

The rhombus **CDEG** forms a spherical four-bar linkage with ground link **CG**, input link **CD**, coupler **DE**, and output link **EG**. The angular lengths of these links are α, β, γ, and η, have the same angular dimension of 35°. The input angle for **CDEG** is denoted Θ and corresponds to the DH angle θ_3. Coupler angle is denoted Φ and corresponds to the DH angle θ_4. Finally, the output angle is denoted Ψ and corresponds to DH angle θ_2. For this linkage, McCarthy and Soh (2011) provide the input-output equation $\Psi(\Theta)$ as,

$$\Psi(\Theta) = \arctan(B,A) \pm \arccos\Big(\frac{C}{\sqrt{A^2+B^2}}\Big), \tag{4}$$

where

$$\begin{aligned} A(\Theta) &= \cos\Theta \sin\alpha\cos\gamma\sin\beta - \cos\alpha\sin\gamma\sin\beta, \\ B(\Theta) &= \sin\Theta \sin\alpha\sin\beta, \\ C(\Theta) &= \cos\eta - \cos\Theta\sin\alpha\sin\gamma\cos\beta - \cos\alpha\cos\gamma\cos\beta. \end{aligned} \tag{5}$$

Furthermore, the coupler angle as a function of the input angle, $\Phi(\Theta)$, is given by,

$$\Phi(\Theta) = \arctan(\sin\Phi, \cos\Phi), \tag{6}$$

where

$$\begin{aligned} \cos\Phi &= \frac{\sin\beta\cos\Theta\cos\gamma\cos\Psi + \cos\Theta\sin\gamma\cos\beta + \sin\beta\sin\Theta\sin\Psi - \sin\alpha\cos\eta}{\cos\alpha\sin\eta}, \\ \sin\Phi &= \frac{-\sin\beta\sin\Theta\cos\gamma\cos\Psi - \sin\Theta\sin\gamma\cos\beta + \sin\beta\cos\Theta\sin\Psi}{\sin\eta}. \end{aligned} \tag{7}$$

From this calculation, we have the joint angle θ_4 as a function of the joint angle θ_3, given by

$$\theta_4 = \Phi(\Theta) = \Phi(\theta_3). \tag{8}$$

The left rhombus **ABCF** is the reflection of the right rhombus **CDEG** relative to the intersection joint **C**. This means the angle θ_3 is the input angle of the spherical four-bar linkage **ABCF**, and the angle $\Psi = -\theta_2$, because it is the reflection of the same angle in **CDEG**. Thus, we have the relations,

$$\theta_2 = -\Psi(\theta_3), \quad \theta_4 = \Phi(\theta_3). \tag{9}$$

This analysis shows that the measured angles θ_1, θ_3, θ_5, yield the angles θ_2 and θ_4, which define the position of the arm measured by the exoskeleton.

4.4. Shoulder RR Model

In order to define the position of the arm of a patient from the matrix $[\mathbf{K}]$ measured by the exoskeleton, we model the shoulder joint as an RR serial chain, where R denotes a revolution. Our RR chain is configured in the same way as the shoulder joint of robot arms such as the PUMA. The DH table of this arm is given in Table 4.

Axis i	Angle ϕ_i	Link offset d_i	Twist $\alpha_{i,i+1}$	Link length $r_{i,i+1}$
1	ϕ_1	0	$\frac{\pi}{2}$	0
2	ϕ_2	0	0	0

Table 4. The DH parameters of the 2R robot on the shoulder joint.

Let $[\mathbf{B_i}]$ denote the homogeneous transformation matrix for each of the two links of our RR shoulder model, then the kinematic equation of the patient's arm relative to the torso is given by

$$[\mathbf{B}(\phi_1,\phi_2)] = [\mathbf{B}_1(\phi_1)][\mathbf{B}_2(\phi_2))] = \begin{bmatrix} \cos\phi_1\cos\phi_2 & -\cos\phi_1\sin\phi_2 & \sin\phi_1 & 0 \\ \sin\phi_1\cos\phi_2 & -\sin\phi_1\sin\phi_2 & -\cos\phi_1 & 0 \\ \sin\phi_2 & \cos\phi_2 & 0 & 0 \\ 0 & 0 & 0 & 1 \end{bmatrix}, \tag{10}$$

where ϕ_1 and ϕ_2 are the angles of the arm along the two rotational axes, which can be regarded as the angle measurement of the shoulder, as shown in Fig. 9.

The measurement of the exoskeleton yields a matrix $[\mathbf{K}]$, which gives us the position of the patient's arm, that is $[\mathbf{T}] = [\mathbf{G}][\mathbf{K}][\mathbf{H}]^{-1}$. In order to determine the angles of the patient's arm using the RR model, we assume

$$[\mathbf{T}] = [\mathbf{B}(\phi_1,\phi_2)], \tag{11}$$

and compute,

$$\phi_1 = \arctan(T_{13}, -T_{23}), \quad \phi_2 = \arctan(T_{31}, T_{32}). \tag{12}$$

This provides an ability to illustrate the position of the arm relative to the coronal, sagittal and transverse plane of the patient, Fig. 9.

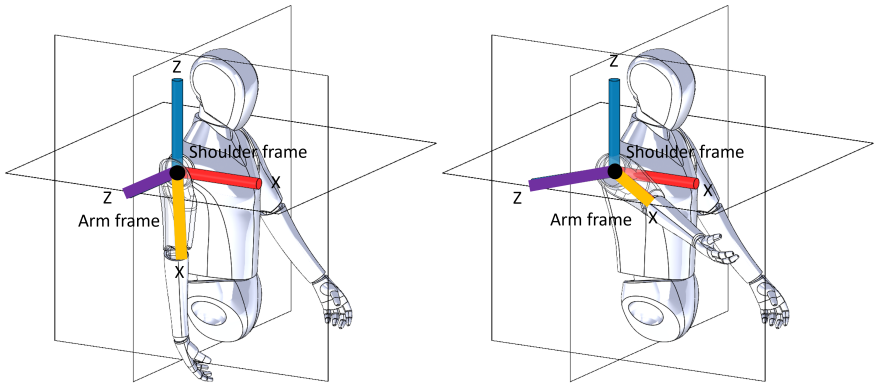

Fig. 9. The two-revolute robotic arm on the shoulder joint showing base frame and end-effector frame. The left figure is the position of initial state. The right figure is the position of flexion 90° and horizontal external rotation 45°.

4.5. Example Calculation

Assuming the natural drooping position of the shoulders as the initial state, the three sensors read zero at this point. The initial DH angles, θ_1, θ_3, and θ_5 for the exoskeleton, are measured from SolidWorks as $-79.94°$, $60°$, and $-123.85°$, respectively. The remaining two angles in the DH table, θ_2 and θ_4, can be obtained from (9) and are found to be $-50.62°$ each. The kinematic equation from the base frame of the

exoskeleton to its end-effector frame is obtained using (3), and then the two transformation matrices [**G**] and [**H**] are measured from SolidWorks by using the dummy model shown in Fig. 9.

$$[\mathbf{G}] = \begin{bmatrix} -0.19 & -0.34 & -0.92 & -113.16 \\ 0.72 & -0.68 & 0.10 & 12.41 \\ -0.66 & -0.65 & 0.38 & 46.52 \\ 0 & 0 & 0 & 1 \end{bmatrix}, \quad [\mathbf{H}] = \begin{bmatrix} 0.99 & 0.13 & -0.10 & -8.90 \\ -0.05 & 0.81 & 0.58 & 49.54 \\ 0.16 & -0.57 & 0.81 & 68.57 \\ 0 & 0 & 0 & 1 \end{bmatrix}, \tag{13}$$

from which we can obtain the kinematic matrix from the base frame to the end-effector frame of the shoulder RR model using (1):

$$[\mathbf{T}] = \begin{bmatrix} 0 & 1 & 0 & 0 \\ 0 & 0 & -1 & 0 \\ -1 & 0.01 & 0 & -0.01 \\ 0 & 0 & 0 & 1 \end{bmatrix}. \tag{14}$$

Using (12), the angles of the shoulder RR model ϕ_1 and ϕ_2 are found to be 0° and -90°, respectively, which match the angles of the shoulder in the initial position.

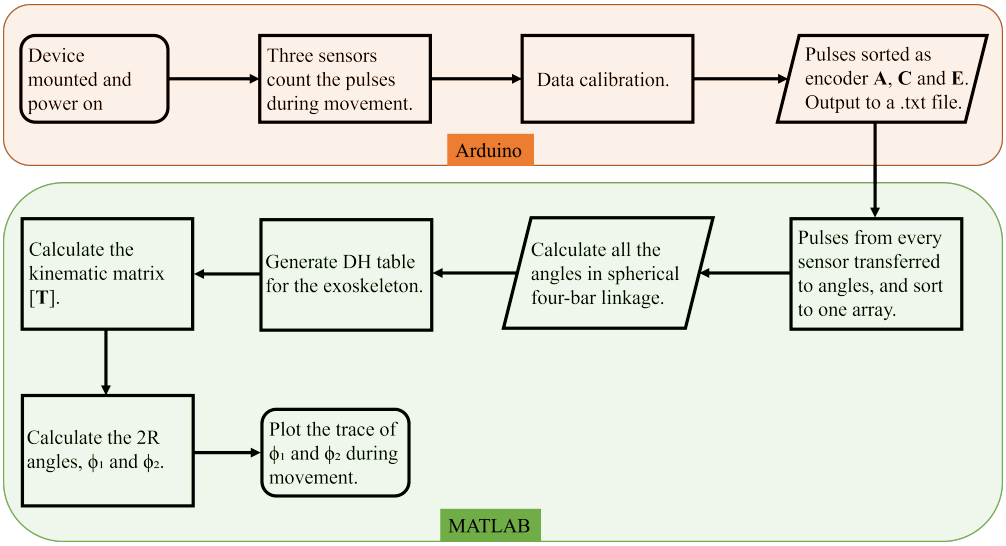

Fig. 10. The encoders **A**, **C**, **E** are read by the Arduino Uno which applies the calibration and outputs joint angle measurements to MATLAB software, which then computes the arm angles.

5. ANALYSIS SOFTWARE

The software on the Arduino Uno counts pulses of the three optical encoders **A**, **C**, **E** and applies the calibration to generate angle measurements. On start-up, the code initializes all angles to 0 degrees, regardless of the angular positions of the exoskeleton. Movement of the joint angles of the exoskeleton are recorded in the Arduino and downloaded to a computer. Data collection is run through the Arduino serial monitor at a baud rate of 500,000, allowing ample time for the large data pool. This data pool is sorted and transferred to MATLAB on the computer. MATLAB software displays the angular measurements at **A**, **C**, **E** over the data collection time period and stores the angle data.

The angles measured at **A**, **C**, **E** define the joint angles θ_1, θ_3 and θ_5 in the kinematics equations **K** of the exoskeleton, (3). The angles θ_2 and θ_4 are calculated from the geometry of the exoskeleton. This matrix **K**

defines the position of the arm measured by the exoskeleton. Once the two transformation matrices [**G**] and [**H**] have been obtained, the rotational angles of the shoulder can be calculated. A comprehensive flowchart is presented in Fig. 10.

6. RESULTS

In order to demonstrate the performance of our spherical shoulder exoskeleton, we measured two positions of a colleague's arm using the device and compared the results to photographs, with angle measurements computed using ImageJ.

Two distinct shoulder movements, flexion and external rotation, were performed and measured using the exoskeleton. The resulting angle measurements are shown in Fig. 11. The flexion angle at the end of flexion movement is measured as $\phi_1 = 80.01^\circ$, and the external rotation angle is measured as $\phi_2 = 24.04^\circ$.

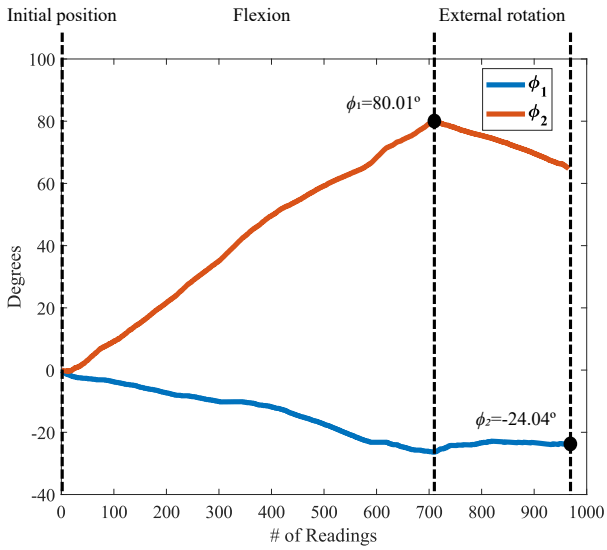

Fig. 11. Calculation results of the two shoulder angles during movements.

Photographs of the positions of the arm in flexion and external rotation are shown in Fig. 12. The measurement of these angles using ImageJ yielded: flexion angle $\phi_1 = 87.04^\circ$, and external rotation angle $\phi_2 = 30.82^\circ$.

The difference between the angles measured by the exoskeleton and the angle measured by photographs and ImageJ are $\Delta\phi_1 = 7.03^\circ$ and $\Delta\phi_2 = 6.78^\circ$.

One important source of error that we found in our experiments is a shifting of the locations for the base and arm attachment of the exoskeleton during testing. Because we rely on the transformations [**G**] and [**H**] defined by these locations, this shifting of position introduces errors. This can be addressed by providing a lighter and lower profile system for carrying the device on the shoulder of the patient.

In a future revision of this prototype, we plan to increase the manufacturing precision of the joints, explore joint designs that increase the encoder range by using small gear trains, and explore a higher performance microprocessor for data acquisition.

7. CONCLUSIONS

This paper presents an instrumented exoskeleton designed to measure shoulder range of movement for assessing performance after surgical replacement of a shoulder joint. The device consists of a spherical

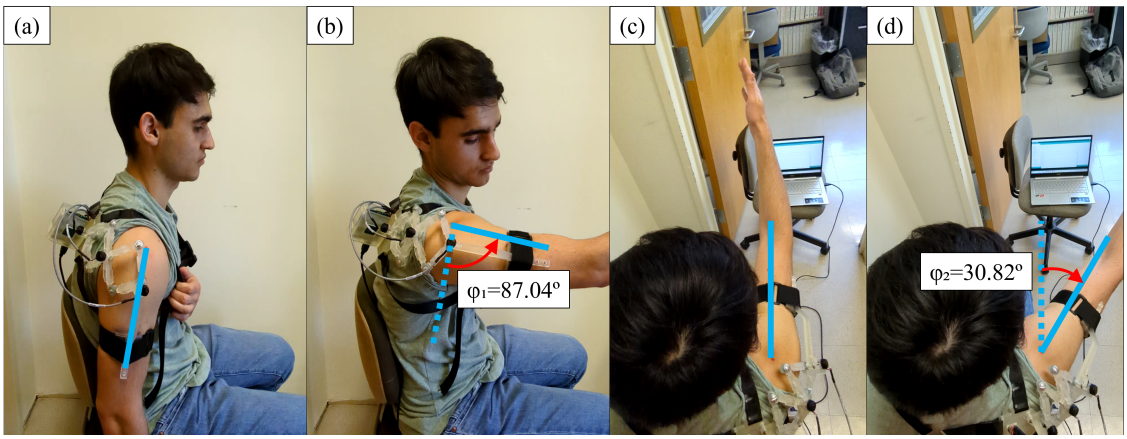

Fig. 12. Pictures of flexion and external rotation test. (a) Initial position, side view, (b) flexion movement, side view, (c) flexion movement, top view, (d) external rotation, top view.

scissor mechanism that is instrumented to measure the position of the upper arm of a patient relative to the torso. We describe the design and fabrication of this device, its calibration, its analysis and verification. The initial results show that our device and photographic measurements are within seven degrees, which is considered to be successful. This error is attributed to movement of the device during testing, which will be addressed in further research.

REFERENCES

1. Castro, M.N., Rasmussen, J., Andersen, M.S. and Bai, S. "A compact 3-dof shoulder mechanism constructed with scissors linkages for exoskeleton applications." *Mechanism and Machine Theory*, Vol. 132, pp. 264–278, 2019.
2. Castro, M.N., Rasmussen, J., Andersen, M.S. and Bai, S. "Compact spherical 3-dof mechanism constructed with scissor linkages." U. S. Patent Application US2020/023854, July 2020.
3. Munoz, G.F., Mollineda, R.A., Casero, J.G. and Pla, F. "A rgbd-based interactive system for gaming-driven rehabilitation of upper limbs." *Sensors*, Vol. 19, No. 3478, 2019.
4. Bilesan, A., Behzadipour, S., Ogawa, S., Tsujita, T., Somizunai, S. and Konno, A. "Marker-based motion tracking using microsoft kinect." *IFAC Papers On Line*, Vol. 51-22, pp. 399–404, 2018.
5. Krishnan, R., Bjorsell, N., Gutierrez-Farewik, E.M. and Smith, C. "A survey of human shoulder functional kinematic representations." *Medical & Biological Engineering & Computing*, Vol. 57, pp. 339–367, 2019.
6. Lenarcic, J., Stanisic, M.M. and Parenti-Castelli, V. "Kinematic design of a humanoid robotic shoulder complex." In "Proceedings of the 2000 IEEE International Conference on Robotics and Automation," , 2000.
7. Gauci, M.O., Olmos, M., Cointat, C., Chammas, P.E., Urvoy, M., Murienne, A., Bronsard, N. and Gonzalez, J.F. "Validation of the shoulder range of motion software for measurement of shoulder ranges of motion in consultation: coupling a red/green/ blue-depth video camera to artificial intelligence." *International Orthopaedics*, 2022.
8. Tanioka, R., Ito, H., Takase, K., Kai, Y., Sugawara, K., Tanioka, T., Locsin, R. and Tomotake, M. "Usefulness of 2d video analysis for evaluation of shoulder range of motion during upper limb exercise in patients with psychiatric disorders." *The Journal of Medical Investigation*, Vol. 69, pp. 70–79, 2022.
9. Park, C. and You, S.H. "Validity and test–retest reliability of an intelligent robotic shoulder joint kinematics system for rehabilitation." *Journal of Mechanics in Medicine and Biology*, Vol. 21, No. 10, 2021.
10. Chiang, C.H. "Spherical kinematics in contrast to planar kinematics." *Mechanism and machine theory*, Vol. 27, No. 3, pp. 243–250, 1992.
11. Hayes, M.J.D., Rotzoll, M., Bucciol, Q. and Copeland, Z.A. "Planar and spherical four-bar linkage vi- vj algebraic input–output equations." *Mechanism and Machine Theory*, Vol. 182, p. 105222, 2023.
12. McCarthy, J.M. and Soh, G.S. *Geometric design of linkages*, Vol. 11. Springer Science & Business Media, 2010.
13. Condino, S., Turini, G., Viglialoro, R., Gesi, M. and Ferrari, V. "Wearable augmented reality application for shoulder rehabilitation." *Electronics*, Vol. 8, No. 1178, 2019.
14. Videogames, U.L.P.R.U.S. and Review, M.C.S.A.S. "Alarcon-aldana, andrea catherine and callejas-cuervo, mauro and bo, antontio padilha lanari." *Sensors*, Vol. 20, No. 5989, 2020.
15. Cubukcu, B., Yuzgec, U., Zileli, R. and Zileli, A. "Reliability and validity analyzes of kinect v2 based measurement system for shoulder motions." *Medical Engineering and Physics*, Vol. 76, pp. 20–31, 2020.

APPENDIX

The Arduino and MATLAB code can be found in this Google Drive folder: `https://drive.google.com/drive/folders/18XZ3T8iQ1MzVMngPpcYfKfxNLCJTCkb_?usp=sharing`.